Environmental Health Perspectives
Vol. 50, pp. 149-161, 1983

Preneoplastic and Neoplastic Progression during Hepatocarcinogenesis in Mice Injected with Diethylnitrosamine in Infancy

by Stanley Goldfarb,*† Thomas D. Pugh,* Hirofumi Koen*‡ and Yu-Zhu He*‡

Basophilic hepatic foci, nodules, and trabecular hepatocellular carcinomas, collectively referred to as focal hepatic lesions, were induced by single injections of 5.0 μg of diethylnitrosamine (DEN) per gram body weight in 15-day-old C57BL/6J × C3HeB/FeJ F_1 (B6C3 F_1) mice. Groups of eight experimental and eight control mice were killed at 3 days and at 1, 2, 4, 10, 20, 28, 36 and 44 weeks after injection. The only observable acute hepatic toxic effect of DEN, a mild steatosis, was noted at 3 days, but this had disappeared by 7 days following injection. Basophilic foci, composed entirely of altered hepatocytes, were first noted, when very small, at 10 weeks. At later times, some of the foci also contained small collections of proliferated ductules, apparently a result of secondary ingrowth from nearby interlobular bile ducts. The hepatocytes within basophilic foci were characterized by their abundant cytoplasmic RNA, a high nuclear to cytoplasmic ratio (two times greater than normal), which gave them a "crowded appearance," and decreased glucose-6-phosphatase activity. During the course of the study, basophilic foci appeared to increase in size and number. Cytologic anaplasia also became more evident, ultimately culminating in the development of typical trabecular hepatocellular carcinomas by 44 weeks. Invasion of hepatic veins by basophilic foci, first noted at 10 weeks, was prominent by 20 weeks and indicated that many of the lesions manifested this characteristic of malignancy well in advance of the anaplastic features that are also diagnostic of hepatocellular carcinoma. The high growth rates of basophilic foci were confirmed by their greatly increased ^{3}H-thymidine labeling indices, which were 20 times greater than background hepatocytes at 20 weeks following DEN injection. Tumor progression during the course of the study was also suggested by a doubling of labeling indices of hepatocytes in the basophilic foci between 20 to 28 weeks. (The term tumor progression is used in a broad biological sense to encompass any or all of the qualitative and quantitative changes describing the stepwise development of initiated cells to highly malignant neoplasms. This definition differs from the more clinical usage which restricts the process to qualitative changes during the late stages in the development of fully autonomous neoplasms.) An analysis of the number and size of transections through basophilic foci and in some cases, actual reconstructions of the foci from serial sections, indicated that, in aggregate, they grew exponentially between 10 to 36 weeks, with a volume doubling time of 2.5 weeks. The combined morphologic and kinetic data support the view that trabecular hepatocellular carcinomas develop from basophilic foci. Because of their ease of quantitation on conventional H&E stained sections, their rather uniformly spherical shapes, and the high probability of their clonal origin, the induced focal hepatic lesions should provide a useful model for studying tumor growth kinetics during carcinogenesis.

*Department of Pathology, University of Wisconsin in School of Medicine, Madison, WI 53706.

†Author to whom requests for reprints should be mailed.

‡Present address: McArdle Laboratory for Cancer Research, University of Wisconsin School of Medicine, Madison, WI 53706.

Introduction

A central problem in characterizing the development of chemically-induced rodent hepatocellular carcinomas is to decide which of the early appearing ductular or hepatocellular alterations are precur-

sors of the carcinomas and which changes are mere epiphenomena. In the rat liver, chemically induced hepatocellular carcinomas are invariably preceded by the development of hyperplastic hepatocellular islands and nodules (*1-5*). On the basis of their often close physical association (*6-8*), their similar histochemical features (*1*, *6*, *9*, 10) and similar growth kinetics (*11*), it appears likely that a small number of hyperplastic lesions undergo tumor progression to hepatocellular carcinomas.

In contrast, tracing the histogenesis of mouse hepatocellular carcinomas has been considerably more problematic. In great part, this has resulted from the difficulty in obtaining general agreement among investigators on the minimal histologic characteristics of hepatocellular carcinomas in this species (*12*). However, this aspect of the problem has now been resolved with the demonstration that single or only few injections of a broad range of carcinogens in infant mice induced a high incidence of metastasizing hepatocellular carcinomas with characteristic trabecular architecture (*3*, *4*). Accordingly, we now thought it timely to analyze the early stages in the development of mouse hepatocellular carcinomas by sacrificing animals at intervals after neonatal injection of a carcinogen, and then histologically and histochemically characterizing and measuring all focal hepatic alterations. Diethylnitrosamine was selected for injection, since single doses of this potent carcinogen induced up to 100% incidence of trabecular hepatocellular carcinomas after 50 to 90 weeks (*15*, *16*). Since the time of tumor initiation is precisely known and the duration between carcinogen treatment and development of carcinomas is apparently very long, then it might be possible to study the kinetics of carcinogen-induced hepatic preneoplastic and neoplastic growth in a similar manner as that reported for the mouse lung adenoma (*17*, *18*) or rat colonic adenocarcinoma (*19*). Furthermore, if easily quantifiable unequivocal premalignant or early-appearing malignant lesions were identified, then the infant mouse liver might also provide a model to rapidly assess and compare the potency of complete carcinogens as well as promoters and inhibitors of carcinogenesis.

Materials and Methods

Male B6C3 F_1 mice were injected IP with 30 μL of saline or with 5.0 μg of DEN/g body weight in the same volume of saline at 15 days of age. Groups of eight experimental and eight control mice were killed at 3 days and after 1, 2, 4, 10, 20, 28, 36 and 44 weeks following injection. The mice that were killed between 3 and 14 days after injection of DEN were injected IP with 0.3 μCi of [methyl-^{3}H] thymidine (New England Nuclear, Boston, MA; specific activity, 7.6 Ci/mmole) 2 hr prior to killing, while those killed at other times were injected IP with 0.6 μCi/g body weight in six divided injections at 6-hr intervals beginning 36 hr prior to sacrifice. The mice were fed *ad libitum* on a mouse chow diet, Teklad 4% mouse and rat diet, (Teklad Standard Diets, P.O. Drawer A, Winfield, Iowa 52659) and they were maintained on a 12 hr light-12 dark cycle (lights off at 6 PM and on at 6 AM) and were killed at 9 AM Sections of liver, measuring about 1 mm in thickness, were taken through the longest axis of each lobe, fixed in formalin for paraffin embedding and frozen for cryostat sectioning.

Paraffin sections cut at 5 μm and cryostat sections that were fixed in formalin were stained with hematoxylin and eosin and by the periodic acid-Schiff staining procedure with and without prior incubation in diastase (*20*). Tissue sections were also stained with toluidine blue, either with or without prior RNAase digestion, to evaluate their RNA content (*20*). Cryostat sections were also stained for alkaline phosphatase (*20*), ATPase (*20*), glucose-6-phosphatase (*21*), and γ-glutamyl transpeptidase activities (*10*, *22*) and for neutral lipids by staining with oil red 0 (*20*).

For the present report, autoradiograms were prepared from paraffin sections of livers (*23*) from mice killed at 20, 28 and 36 weeks. Tritiated thymidine; (^{3}H-Tdr) labeling indices were determined in focal hepatocellular lesions and in background hepatocytes. All labeled and unlabeled cells were counted at 100× after superimposing a 250 × 250 μm grid over the observed field. For focal hepatocellular lesions having diameters measuring less than 700 μm, labeling indices were based on study of all cells. However, to avoid counting cells that might have suffered ischemic injury, only cells at the peripheries of the lesions that were larger than 700 μm in diameter were evaluated. The nuclear to cytoplasmic ratios of hepatocytes in focal lesions, in nonneoplastic background liver and in control liver were measured by employing the point-counting technique of Chalkley (*22*).

The areas of profiles of focal hepatic lesions and of liver sections were determined by projecting their magnified images, drawing their outlines on paper, and either weighing the properly calibrated cut out sections of integrating their areas by computer-assisted planimetry (*23*). [A profile is defined as a projection of a three-dimensional object on a plane (*3*).] Since most of the focal lesions appeared roughly circular in tissue sections, it was decided to assess the degree of sphericity in two blocks of liver from mice killed at 10 and 20 weeks. The exact volumes of 26 randomly selected

basophilic foci were then determined from serial section reconstruction and compared to those areas of their largest cross-sectional (presumably equatorial) profiles. For this study and another one in which the total numbers of foci in measured volumes of liver were to be determined (see Results), approximately 200 sections, 5 μm thick, were serially cut from 1 mm thick blocks of paraffin-embedded liver. The sections were then stained with hematoxylin and eosin, and the cross-sectional areas of tissue sections and profiles of focal lesions were determined. The volumes of the focal lesions were then determined by summing their volumes in the individual sections, and the volumes of liver were determined by interpolation after measuring the areas of every tenth section.

During the course of the study, it was discovered that flotation of paraffin-embedded tissue sections on the water bath resulted in a highly reproducible 20% increase in cross-sectional area of the liver tissue. This necessitated a proportionate reduction of all area measurements for accurate quantitation.

Results

Body and Liver Weights in Control and Experimental Animals

Major increases in body and liver weights in control and experimental animals occurred prior to the tenth week after injection. The mean body weights of both groups of animals increased to 25 g at 20 weeks after diethylnitrosamine and were essentially unchanged throughout the remainder of the study. In control animals, the mean liver weight had reached about 90% of its maximum by 10 weeks and it, too, remained quite constant at about 1.25 g at 20 weeks and later (Fig. 1). The weights of the livers were similar in control and experimental animals until 28 weeks after carcinogen treatment. After that time, due to enlargement of neoplasms, the livers of carcinogen-treated mice underwent marked increases in weight. They were 26% heavier than controls by 36 weeks and twice the mean control weight by 44 weeks.

Hepatic Changes during the First Four Weeks

Lipid accumulation was prominent in central and midzonal areas of hepatic lobules by 3 days after DEN injection, but these changes had completely regressed after an additional 4 days. At no time were fatty changes observed in control mice. Glycogen was not demonstrable by periodic acid-Schiff stain in the control or experimental livers, and enzyme histochemical patterns also did not differ in experimental and control sections. In this regard, glucose-6-phosphatase activity had a predominantly periportal distribution; ATPase activity was minimal and limited to canaliculi; alkaline phosphatase activity showed only minimal activity in canaliculi and plasma membranes bordering liver sinusoids; and γ-glutamyl transpeptidase activity was not demonstrable in hepatocytes.

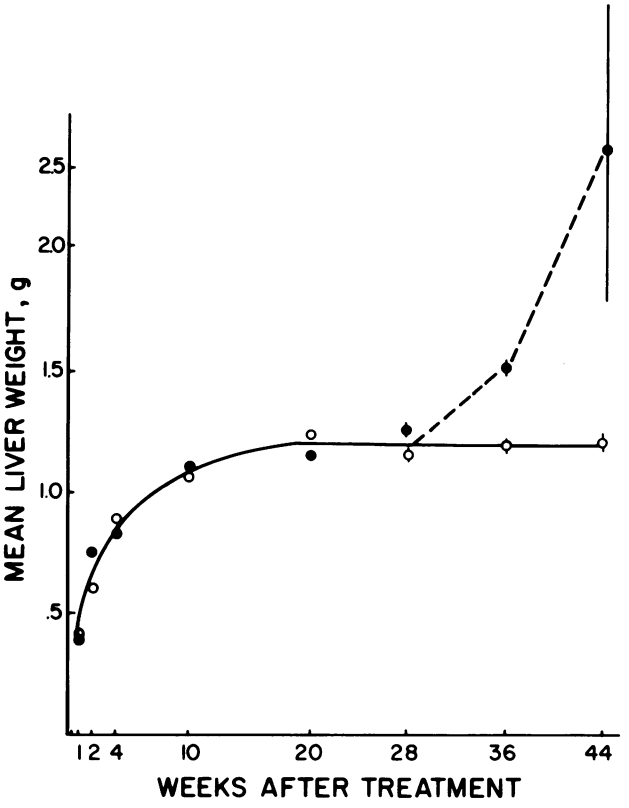

FIGURE 1. Mean liver weight at sacrifice of (o) control mice and (•) mice injected with diethylnitrosamine. Means ± SEM are shown at 28, 36 and 44 weeks after injection.

Hepatic Changes between 10 and 44 Weeks

Morphological Features. Distinctive collections of cells, referred to as basophilic hepatic foci and nodules, were the only alterations in addition to late-appearing (44 weeks) trabecular hepatocellular carcinomas that were identified in the livers of mice killed during this period. At 10 weeks after injection, the foci were infrequent, very small, and composed entirely of basophilic hepatocytes (Fig. 2). However, after that time focal hepatic lesions were more numerous and showed a progressive increase in size (Figs. 3-6). On randomly cut sections, the vast majority of these also contained only hepatocytes. However, when cut serially, some of the larger foci contained relatively small well-

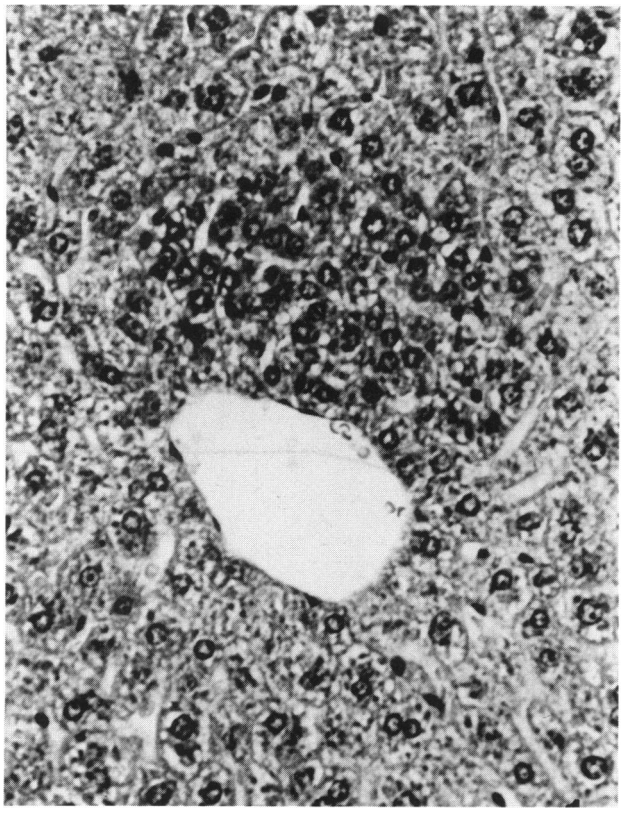

FIGURE 2. Tiny basophilic hepatic focus adjacent to a terminal hepatic vein. The high nuclear to cytoplasmic ratio results in a "crowded" appearance. The mouse was killed 10 weeks after injection of diethylnitrosamine. H&E. × 380.

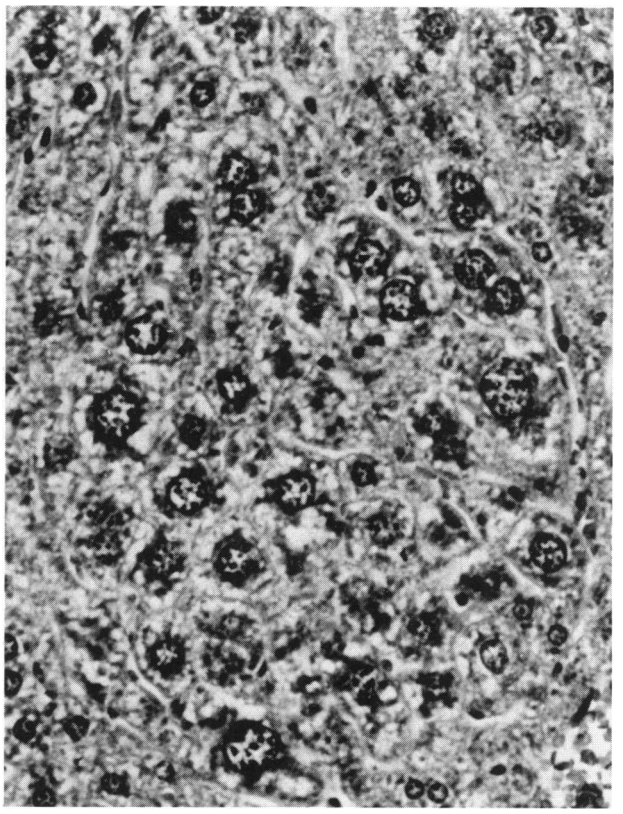

FIGURE 3. A tiny basophilic hepatic focus containing cells with relatively large nuclei. The high nuclear to cytoplasmic ratio is still apparent. The mouse was killed 20 weeks after diethylnitrosamine injection. H&E. × 380.

delineated aggregates of proliferated bile ductules in addition to the hepatocytes (Figs. 4 and 5). Invariably, these clusters of proliferated ductules were found connected to interlobular bile ducts which entered the foci in association with "feeding" portal vein branches at their peripheries (Figs. 4 and 5). In addition to their basophilia, the hepatocytes within the foci showed a characteristic "crowding" of cells which resulted from their high nuclear to cytoplasmic ratios (Figs. 2 and 3) and from their growing in sheets. The latter change has been attributed to a collapse of the sinusoids (24). Although most of the hepatocytes were smaller than normal (Fig. 3), some appeared enlarged (Fig. 2). In either case, however, the high nuclear to cytoplasmic ratio was evident.

The outlines of the foci profiles appeared to vary with their sizes. The smallest profiles were sometimes irregular with oval or even triangular shapes, while the remainder, particularly the largest ones, were almost circular (Figs. 3, 5 and 6). Because of the "crowding" of cells with basophilic foci, it was often difficult to determine the thickness of hepatic plates. When discernible, however, they were predominently one to two cells in thickness (Fig. 7). Infiltration into small hepatic veins was a prominent characteristic of the basophilic foci (Fig. 8). Although rarely present in foci from mice sacrificed at ten weeks, it was very common at 20 weeks and later. In fact, in one serially sectioned block of liver from a 20 week mouse, nine of 45 identified foci were found to infiltrate the hepatic veins. In contrast, portal veins were not invaded. The preferential invasion of hepatic veins was of particular interest, since smaller foci often seemed to be located closer to the terminal hepatic veins than to the portal vein branches (Fig. 2).

A few grossly visible nodules, with the histologic features of foci and measuring up to 2 mm in diameter, were first noted in mice sacrificed at 36 weeks after injection. By 44 weeks, these had become more frequent, showing further enlargement, and in

FIGURE 4. Basophilic hepatic focus showing entry of a small portal vein branch and bile duct at its lower margin. The outlined area is shown at higher magnification in Fig. 5. The mouse was killed 28 weeks after diethylnitrosamine injection. H&E. × 195.

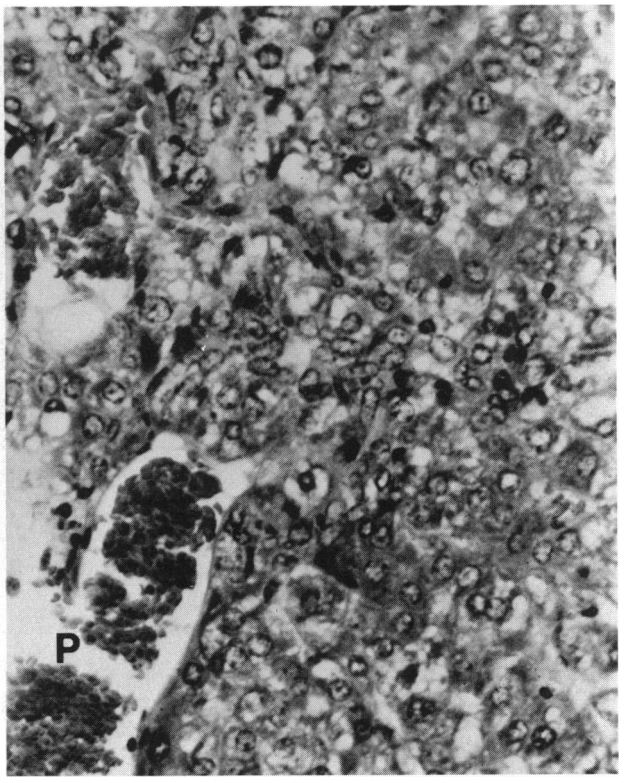

FIGURE 5. Prominent ductular cell proliferation in the region above the point of entry of the portal vein branch (P). H&E. × 380.

a few instances, manifested more marked cytologic atypia and further thickening of hepatic plates (four to five cells) characteristic of trabecular hepatocellular carcinomas (Fig. 9). Mitoses were not identified in any of the basophilic foci from mice sacrificed up to 20 weeks, but they were abundant within some basophilic foci and all trabecular hepatocellular carcinomas after that time (Fig. 10).

Hepatocytes within foci from mice killed at 10 and 20 weeks appeared quite homogeneous, despite some variation in nuclear and cell sizes. Beginning at 28 weeks, however, and also noted at later times, there was often a distinctive zonal heterogeneity within the larger focal hepatic lesions (Fig. 6). While the cells in the peripheries of the focal lesions continued to show a characteristic cytoplasmic basophilia and high nuclear to cytoplasmic ratio, those located in the deeper regions often appeared eosinophilic or hydropic, and, at times, even contained neutral lipid and showed frank necrosis. These changes were particularly prominent in the more anaplastic trabecular carcinomas.

Histochemical Features of Hepatocytes in Basophilic Foci. The cytoplasmic basophilia in the foci resulted from accumulation of RNA, since it was totally eradicated by incubation with RNAase prior to staining with toluidine blue. An additional histochemical alteration, seen in all basophilic foci, was a deficiency of glucose-6-phosphatase (Figs. 11 and 12). The regularity of this enzymatic change deserves particular emphasis. Without exception, every one of 100 cryostat-cut basophilic foci from mice sacrificed at 10 and 20 weeks after carcinogen injection showed marked or complete loss of cytoplasmic glucose-6-phosphatase activity. The distributions of other enzyme histochemical activities, including ATPase, alkaline phsophatase and γ-glutamyl transpeptidase were no different from those in the controls. Just as the earlier times, glycogen was absent from the foci and from the surrounding hepatocytes.

Nuclear to Cytoplasmic Ratios of Hepatocytes in Basophilic Foci. The nuclear to cytoplasmic ratios in foci from livers of mice injected with

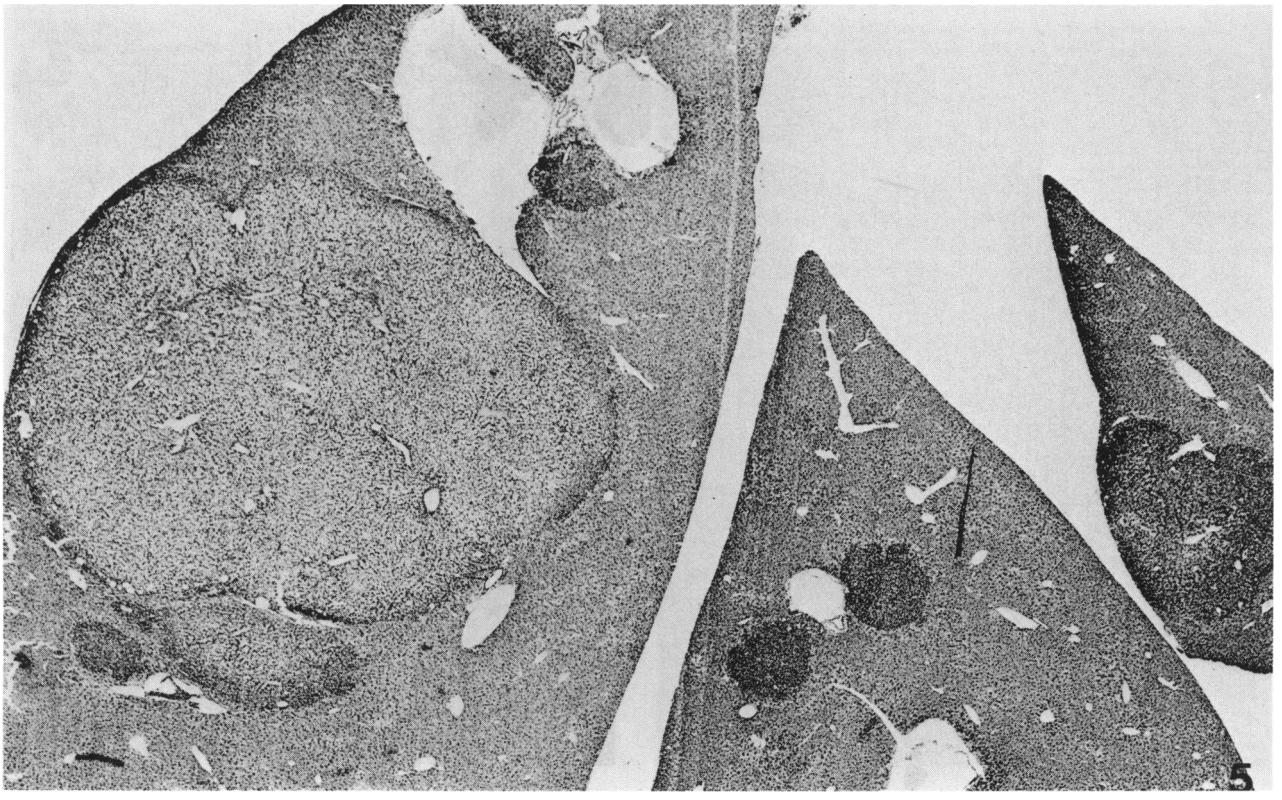

FIGURE 6. Multiple basophilic hepatic foci in the liver of a mouse killed 36 weeks after diethylnitrosamine injection. The largest focus on the left has a pale interior due to hydropic changes and neutral lipid accumulation. However, the peripheral hepatocytes retain a basophilic appearance. H&E. × 20.

diethylnitrosamine 10 or 20 weeks earlier, were consistently and significantly increased when this parameter was compared to adjacent background hepatocytes or to hepatocytes from control livers (Table 1). At each sacrifice time, the ratios were about two times higher in the foci than in the comparable control tissue.

Shape of Basophilic Foci. A particularly good correlation (r = 0.99) was demonstrated between the maximal cross-sectional areas of foci, presumed to be through their equatorial planes, and the volumes of the foci (Fig. 13). Since the line depicting this experimentally derived relationship was very close to and almost parallel to the line showing the correlation between spheres and their largest cross sectional areas, it appeared reasonable to conclude that most foci had almost spherical shapes.

Quantitation of Size, Number, and Volumes of the Basophilic Hepatic Foci. In order to compare the number and sizes of basophilic hepatic foci at different sacrifice times, serially sectioned blocks of liver from several mice were compared. For this study it was sufficient to identify and determine the largest cross sectional area of the foci, since this parameter provides a close approximation of the foci volumes. This was accomplished by first identifying all foci and then for each, determining the five or six largest cross sectional areas planimetrically. The single largest transection was then readily selected. Data for two of the livers, one at 20 weeks and one at 28 weeks post-carcinogen injection, are indicated in Figure 14 and Table 2. As noted, the two mice, selected for comparison, had almost identical total numbers of foci, but the 28 week mouse liver had three times more foci (12% of the total) in the four largest size classes than the 20 week mouse liver (4% of the total). This small increase in the absolute number of larger foci resulted in a very great increase (7-fold) in the aggregate volume of all the foci. The effect of these larger foci on the total number of transections is also apparent in Figure 14. Clearly, the larger foci generated more profiles in the tissue sections. Thus, despite a similar number of foci, the liver from the 28 week old mouse contained almost twice as many profiles as that from the 20 week mouse. These examples were useful for

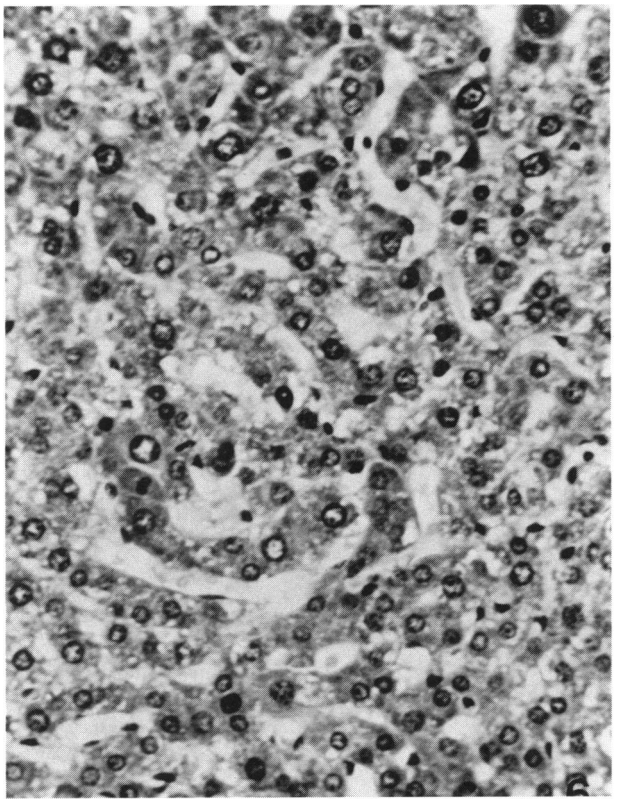

FIGURE 7. Hepatocytes in the center of a basophilic hepatic focus showing one cell thick plates. The mouse was killed 20 weeks after diethylnitrosamine injection. H&E. × 380.

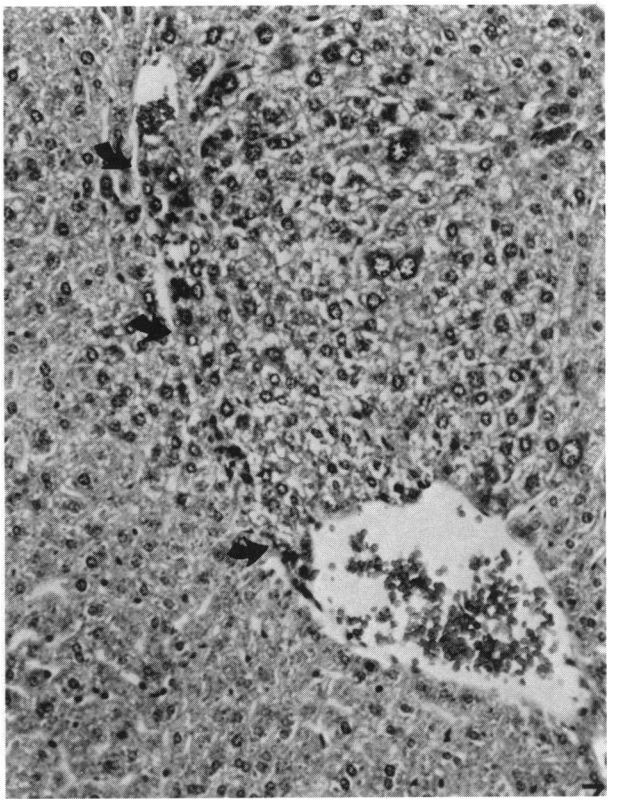

FIGURE 8. Basophilic hepatic focus that has infiltrated a small hepatic vein branch. A tumor thrombus (arrows) fills approximately one half of the lumen. The mouse was killed 20 weeks after diethylnitrosamine injection. H&E. × 195.

interpreting the profile data from the livers of groups of animals sacrificed at each of four time points (Fig. 15 and Table 3). Because of the almost 10-fold increase in the number of profiles between 10 and 36 weeks, it appears very likely, although not proven, that the absolute number of foci increased during this interval. The evidence for progressive enlargement of the foci is more impressive, since the number of profiles in the largest size class (64,000 μm^2) showed significant increases with time. The effect of the progressively increasing number of large foci on the total volume of the tumors may be deduced from Figure 15, which depicts an exponential increase with time in the fraction: profile areas/sections areas. Since the liver weights showed only slight increase after 10 weeks, and since the ratios between areas are proportional to the ratios between volumes (26), it follows that, in aggregate, the foci volumes also showed exponential increases during the interval under study.

Labeling Indices of Foci. As a further measure of growth rate, the ^{3}H-Tdr labeling indices were determined for most of the foci at 20 weeks, and for a comparable number of randomly selected foci at 20 and 36 weeks after diethylnitrosamine injection. The cumulative data (Table 4) demonstrated a 10- to 80-fold increase in mean labeling indices in the foci when compared to normal-appearing (background) areas within the experimental livers. The mean labeling index was 1.6% after 20 weeks, and underwent a further increase to 3.7% at 28 weeks. The labeling indices remained at this high rate (3.2%) in mice sacrificed at 36 weeks after injection. The increase in labeled cells was not restricted to foci from particular livers since it was documented, to a similar degree, in foci from all livers. The presence of mitoses in some of the foci in mice killed after 20 weeks appeared to correlate with the increase in the mean labeling index that occurred at that time.

Discussion

This report documents the early homogeneous appearance and progressive changes in foci of hepatocytes that appeared after a single injection of di-

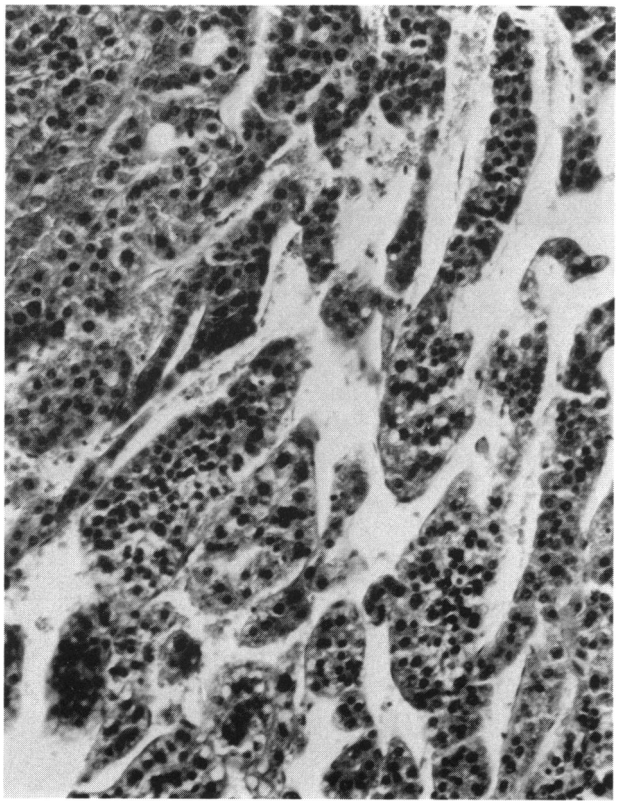

FIGURE 9. Trabecular hepatocellular carcinoma showing papillary features and marked anaplasia in a mouse that was killed 44 weeks after diethylnitrosamine injection. H&E. × 195.

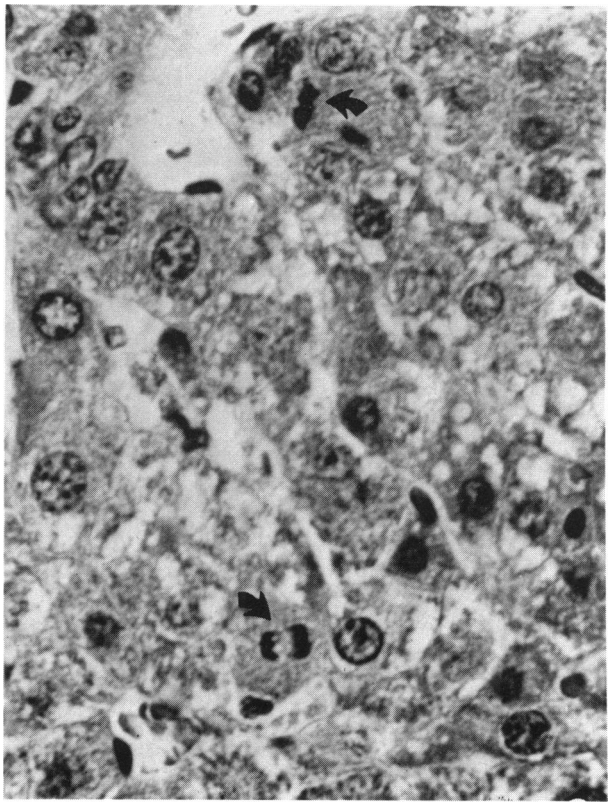

FIGURE 10. Mitotic figures (arrows) in a basophilic hepatic focus from a mouse killed 36 weeks after diethylnitrosamine injection. H&E. × 760.

ethylnitrosamine in infant mice. The smallest foci, first noted at 10 weeks following carcinogen treatment, were composed of hepatocytes showing high nuclear to cytoplasmic ratios, diminished or absent glucose-6-phosphatase activity, and increased cytoplasmic RNA. In many organs, an increase in nuclear to cytoplasmic ratio is generally considered a feature of premalignant and malignant cells (*25*), and in rat liver, the focal loss of glucose-6-phosphatase activity characterizes a subset of putative premalignant hepatocellular islands (*1,8,9*). The malignant and premalignant character of the early foci is also supported by the finding that some of them were found to invade terminal hepatic veins as early as ten weeks following injection of diethylnitrosamine. Indeed, the early invasive character of the foci appears to correlate quite well with the late appearance, in high incidence, of pulmonary metastases (*15,16*).

After 10 weeks, the focal lesions enlarged, became more anaplastic, and further increased their already high thymidine labeling indices. Since tumor progression is accompanied by a process of selection in which the most rapidly replicating or longer lived cells tend to overcrowd the remaining cells, one might expect to see a progressive increase with time in the growth rates of tumors (*26*). However, one note of caution should be sounded. Since we did not correlate labeling indices with sizes of foci, we cannot exclude the possibility that the indices are related more to the number of cells in foci than to the duration following carcinogen treatment. Despite this limitation, the temporal evidence for tumor progression is compelling, and it appears that the uniform early basophilic foci developed into trabecular hepatocellular carcinomas by a stepwise or sequential process similar to that suggested for diverse neoplasms (*27*).

During the course of this study, the aggregate volume of the focal lesions increased exponentially in a fashion that suggests the early growth phase of autonomous neoplasms (*28*). Of course, the observed aggregate tumor doubling time of 2.5 weeks is only an average of the growth rates of all the focal le-

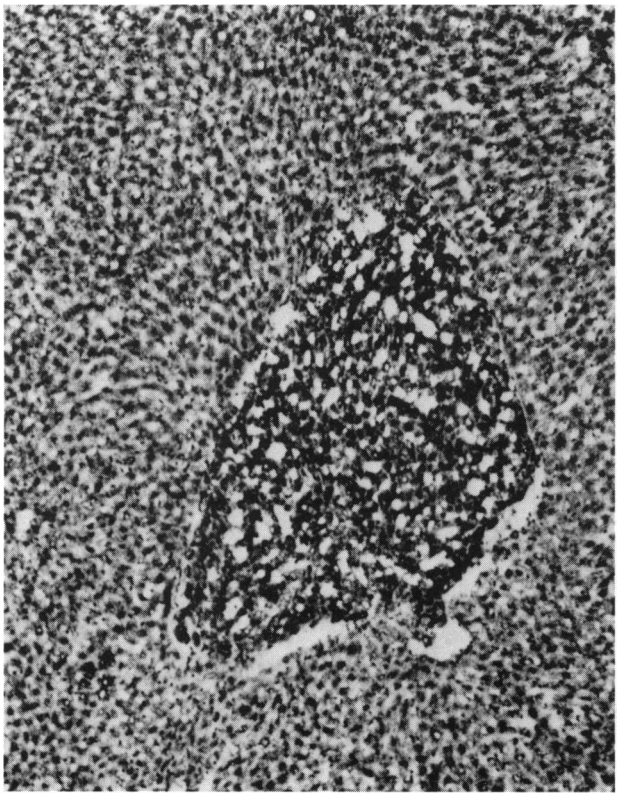

FIGURE 11. Serial cryostat section showing a basophilic hepatic focus from a mouse killed 20 weeks after diethylnitrosamine injection. × 83. Toluidine blue stain showing intense basophilia of the focus.

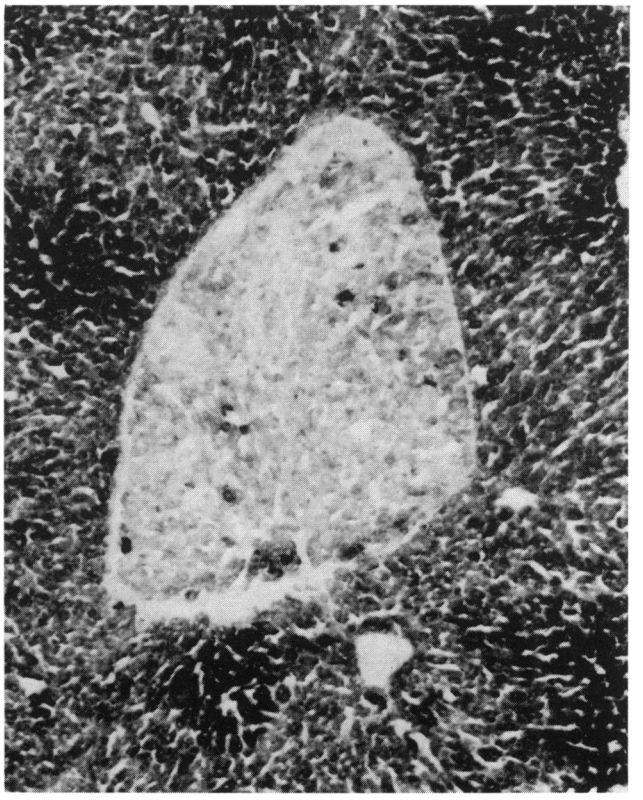

FIGURE 12. Section as in Fig. 11 stained for glucose-6-phosphatase activity. The focus is almost devoid of enzyme activity.

Table 1. Nuclear to cytoplasmic ratios (N/C) of hepatocytes in basophilic hepatocellular foci, background areas and control livers.

Time after DEN injection, weeks	Number of experimental mice	N/C ratios		
		Foci	Background areas[a]	Control areas
10	3	0.115 ± 0.042 (6)[b,c,d,e]	0.055 ± 0.011 (6)	0.054 ± 0.013 (16)
20	8	0.140 ± 0.048 (40)	0.070 ± 0.017 (16)[f]	0.068 ± 0.016 (16)[g]

[a] Background areas represent normal appearing hepatocytes in livers that also contained basophilic hepatocellular foci.
[b] Number in parentheses = number of hepatocellular foci or number of microscopic fields of normal hepatocytes.
[c] Mean ± standard error of the mean for this and subsequent tables.
[d] Differences between N/C ratios in 10 week foci vs. background areas. $p<0.01$ Student's t-test for this and subsequent tables.
[e] Differences between N/C ratios in 10 week foci vs. control areas. $p<0.002$.
[f] Differences between labeling indices in 20 week foci vs. background areas and between 20 week foci and control areas. $p<0.002$.

sions. In fact, the effect of only a few large foci was evident in the serial section study of two livers from mice killed at 20 and 28 weeks. In both cases, the foci were spread through a very broad range of sizes, and only about 10 to 15% of them accounted for approximately 90% of the tumor volume. The two mice had almost identical numbers of foci, but a small fraction of the total were considerably larger in the older mouse. This resulted in a 7-fold greater aggregate tumor volume and clearly indicates that future kinetic analyses will require accurate assessment of the size distributions of foci. In our most recent study, we have determined that at 10 weeks, the five largest foci contained an average of about 1000 cells each (H. Koen, S. Goldfarb, T. D. Pugh, Y. Z. He, and S. D. Vesselinovitch, unpublished ob-

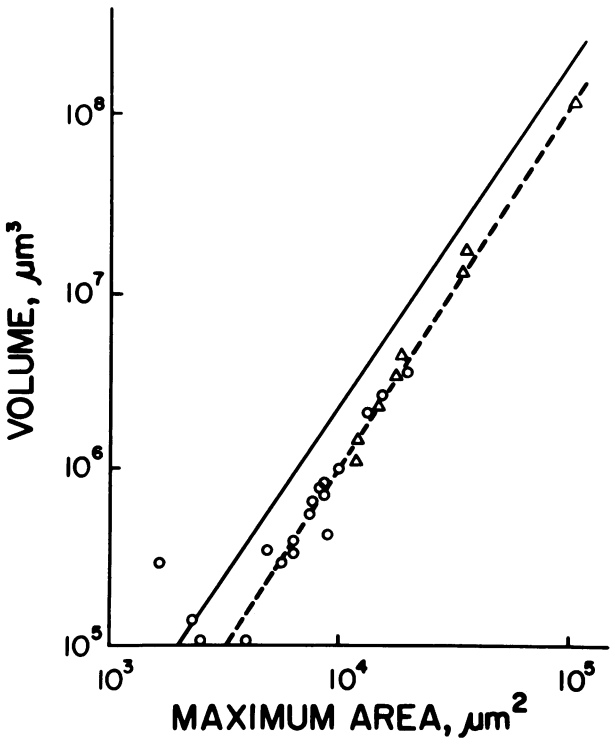

FIGURE 13. Plot depicting the correlation between the maximal cross sectional areas and volumes of individual foci. (△) data from mice killed 20 weeks after diethylnitrosamine injection; (○) similar data from mice killed 10 weeks after injection; (——) relationship between the volumes of perfect spheres and the areas of circular profiles through their equatorial planes. The data were derived from serial section reconstructions. Correlation coefficient r = 0.99.

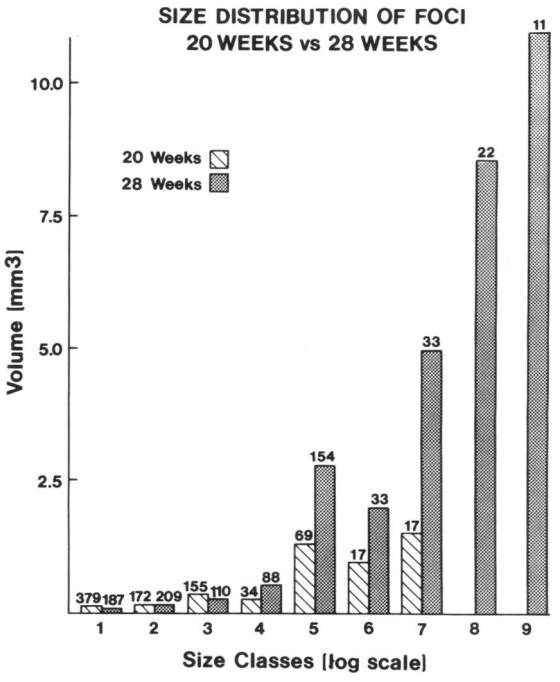

FIGURE 14. Histogram of foci size distribution in two mice killed at 20 and 28 weeks. The size classes denote the largest cross sectional areas of the foci and increase exponentially through nine size ranges. For example, size class 1 includes all foci having largest cross-sectional areas between 5,000 and 10,000 μm^2 and size class 2 includes all foci between 10,000 and 20,000 μm^2, etc. The largest size class (class 9) includes all foci whose largest cross sectional areas measure between 1.28 and 2.56 mm^2. The numbers above the bars refer to the number of foci in the particular size class, while the height of the bar indicates the total volume contribution of all foci in that size class. The data are summarized in Table 2.

servations). If one assumes, on the basis of their origin from previously normal livers and their spherical shapes, that each focus arose from a single cell, then the doubling time of these selected foci during the first ten weeks was about one week.

Hepatic foci induced by carcinogen injection in infant mice are probably better suited for accurate assessment of tumor cell kinetics than are other currently available in vivo models for hepatocarcinogenesis. Recently, mathematical formulas (*5,29*) and "best-curve-fits" (*30*) have been applied to an analysis of random transections of hepatocellular foci and other three-dimensional structures in order to determine the approximate number of these objects in a tissue or organ. However, accurate estimation necessitates large numbers of transections and mathematically defineable shapes of the objects (*30,31*). Until now, the degree of uniformity of the three-dimensional shapes of preneoplastic or neoplastic foci had not been assessed in any model for hepatocarcinogenesis. This could be a significant oversight for studies conducted in the rat since the putative preneoplastic foci, even late in the course of carcinogenesis, sometimes showed quite irregular shapes (*8*). In addition, in some studies, the macroscopic nodules, presumably derived from islands, were reported to undergo regression or remodeling after discontinuation of the carcinogen (*9,32,33*). Ogawa et al. (*30*) have clearly detailed the remodeling phenomenon which may result in at least some "islands" being derived from nodules; it could also account, in

Table 2. Comparison of the total number of foci, profiles and their aggregate volumes in livers of two mice killed at 20 and 28 weeks.[a]

	20 weeks	28 weeks
Total number of foci/cm^3	845	846
Foci profiles/cm^2	8.9	16
Total volume of foci, mm^3/cm^3	4.5	31

[a] Summary of data shown in Fig. 14.

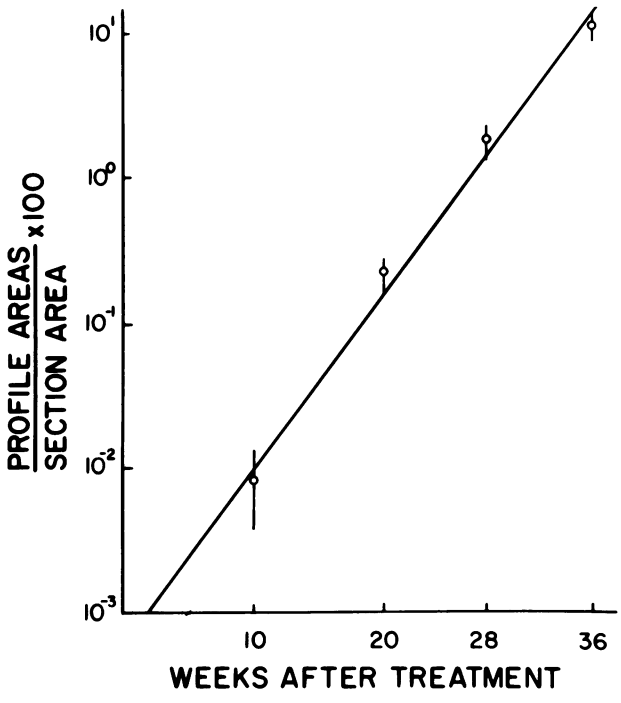

FIGURE 15. Percentage of section areas occupied by profiles of hepatocellular foci in sections from livers of mice injected with DEN. The plotted data points are means ± SEM for groups of eight mice at each sacrifice time. Correlation coefficient r = 0.99.

part, for the irregularity in the shape of islands. In contrast, the mouse foci maintained close-to-spherical shapes, a feature that enabled us to directly extrapolate from their largest cross-sectional areas to the foci volumes. Furthermore, the round shapes and sharp demarcation of the mouse foci strongly suggests that they do not undergo regression.

Recently, there has been considerable interest in distinguishing spontaneous from carcinogen-induced mouse hepatocellular nodules by cytologic criteria. It has been suggested that the cells comprising spontaneous hepatocellular neoplasms are generally basophilic, while those induced by carcinogens are more frequently eosinophilic (*34*). Our findings are not consistent with this hypothesis, since all hepatocytes in the earlier appearing small foci and the peripheral well-perfused hepatocytes of the large focal lesions had basophilic cytoplasms. However, these results certainly do not rule out a malignant or premalignant role of the eosin-stained hepatocytes. On the contrary, cells of this type, with abundant cytoplasm often make up the majority of foci and nodules induced by chronic treatment with carcinogen (*35-37*). There is good reason to consider some of them as precursors of trabecular carcinomas, since they appear early (*35,37*) and are often found intermixed in nodules containing trabecular hepatocellular carcinomas (*36*). Also, in one report, they were

Table 3. Number of foci profiles per square centimeter in livers of mice at intervals after diethylnitrosamine injection.

	No. of mice	Average no. of profiles per cm²	Number of profiles in various size classes			
			0.5-4 × 10^{-4} mm²	4-16 × 10^{-4} mm²	16-64 × 10^{-4} mm²	64 × 10^{-4} mm²
10 weeks	8	2.68	2.55 ± 0.66	0.13 ± 0.14	0	0
20 weeks	8	9.25	6.41 ± 0.96	1.98 ± 0.88	0.61 ± 0.44	0.25 ± 0.26*
28 weeks	8	12.80	4.89 ± 1.33	2.41 ± 0.75	3.42 ± 1.04	1.24 ± 0.56**
36 weeks	8	25.73	6.26 ± 0.71	6.36 ± 2.27	5.48 ± 0.58	7.63 ± 1.48

* Difference between the number of profiles in this size class at 20 and 28 weeks, $p<0.005$.
** Difference between the number of profiles in this size class at 28 and 36 weeks, $p<0.001$.

Table 4. ^{3}H-Tdr labeling indices in livers of mice at intervals after diethylnitrosamine injection.

Time after injection, weeks	No. of mice	Types of sampled areas	No. of foci or areas[a]	Labeling indices[b]
20	6	Foci	28	1.62 ± 0.35*†
		Background	154	0.08 ± 0.03
28	8	Foci	34	3.73 ± 0.39
		Background	427	0.32 ± 0.03
36	8	Foci	49	3.22 ± 0.27
		Background	383	0.04 ± 0.01

[a] Background areas were randomly sampled fields (62,500 μm²) of normal appearing hepatocytes from the experimental livers. Each field contained approximately 100 cells.
[b] Mean ± SEM.
* Difference between labeling indices in 20 vs. 28 week mice and 20 vs. 36 week mice. $p<0.002$.
† Differences between labeling indices in foci and their comparable background areas. $p<0.0001$.

found to have a rate of replication intermediate between normal hepatocytes and carcinoma cells and both they and the carcinoma cells acquired an oncofetal antigen associated with plasma membranes (*37*). Thus, for the present, we suggest that carcinogen-induced premalignant foci could have either type of staining characteristic. Perhaps the difference in staining between the early foci relates more to the duration of carcinogen treatment, since the eosinophilic staining quality is often a consequence of adaptive hyperplasia of the endoplasmic reticulum, in response to chronic exposure to a toxic substance (*12*).

One additional histologic features warrants comment. We found small clusters of bile ductules within some basophilic hepatic foci during the late course of carcinogenesis. Similar clusters, referred to as oval cells, have been identified in hepatic neoplasms induced by an organic phosphorous insecticide (*38*). The possibility that these lesions are precursors of the basophilic hepatic foci must therefore be considered (*39*). However, bile ductules were not found in the earliest foci, and even when present in the larger foci, they invariably connected to peripheral bile ducts. Consequently, we believe that proliferation of bile ductules is probably of no histogenetic significance but that it reflects a secondary response to enlarging focal hepatocellular lesions.

After this manuscript was completed and our own results had already been reported (*40,41*), a paper was published that independently confirmed several of our own findings (*42*). Moore et al. found that when B6C3 F_1 and CD-1 mice were injected at birth with a dose of diethylnitrosamine that was four times greater than the one we used, they too induced basophilic hepatocellular foci that were deficient in glucose-6-phosphatase activity. Again, as in our study, these investigators reported a progressive increase with time in the size of the focal lesions.

We thank Dr. Stan D. Vesselinovitch and his associate, Dr. N. Mihailovich, of the Departments of Radiology and Pathology at the University of Chicago, for providing us with the treated and control mice used in this study.

The superb technical assistance of Mrs. Donna Pearce is gratefully acknowledged.

This study was supported by NIH Grants CA15664 and CA25522. This study was carried out during the tenure of Dr. Pugh on NIH Postdoctoral Fellowship 1-F32-CA15785.

REFERENCES

1. Gossner, W., and Friedrich-Freksa, H. Histochemische Untersuchungen uber die Glucose-6-phosphatase in der Rattenleber wahrend der Kanzerisierung durch Nitrosamine. Z. Naturforsch. 19B: 862-863 (1964).
2. Kinosita, R. Studies on the carcinogenic chemical substances. Trans. Japan. Pathol. Soc. 27: 665-727 (1937).
3. Sasaki, T., and Yoshida, T. Experimentelle Erzeugung des Lebercarcinoms durch Futterung mit *o*-Aminoazotoluol. Virchows Arch. Pathol. Anat. Physiol. Klin. Med. 295: 175-200 (1935).
4. Schauer, A., and Kunze, E. Enzyme Histochemische und autoradiographische Untersuchungen wahrend der Cancerisierung der Rattenleber mit Diethylnitrosamine. Z. Krebsforsch. 70: 252-266 (1968).
5. Scherer, E., and Emmelot, P. Kinetics of induction and growth of precancerous liver-cell foci, and liver tumor formation by diethylnitrosamine in the rat. Eur. J. Cancer 11: 689-696 (1975).
6. Farber, E. The pathology of experimental liver cell cancer. In: Liver Cell Cancer (H. M. Cameron, D. A. Linsell, and G. P. Warwick, Eds.), Elsevier Publishing Co., Amsterdam, 1976, pp. 243-257.
7. Goldfarb, S. A Morphological and histochemical study of carcinogenesis of the liver in rats fed 3′-methyl-4- dimethylaminoazobenzene. Cancer Res. 33: 1119-1128 (1973).
8. Pugh, T. D., and Goldfarb, S. Quantitative histochemical and autoradiographic studies of hepatocarcinogenesis in rats fed 2-acetylaminofluorene followed by phenobarbital. Cancer Res. 38: 4450-4457 (1978).
9. Goldfarb, S., and Zak, F. G. Role of injury and hyperplasia in the induction of hepatocellular carcinoma. J. Am. Med. Assoc. 178: 729-731 (1961).
10. Kelengayi, M. M. R., Ronchi, G., and Desmet, V. J. Histochemistry of gamma-glutamyl transpeptidase in rat liver during aflatoxin B_1-induced carcinogenesis. J. Natl. Cancer Inst. 55: 579-588 (1975).
11. Kunz, W., Appel, K. E., Rickart, R., Schwarz, M., and Stockle, G. Enhancement and inhibition of carcinogenic effectiveness of nitrosamines. In: Primary Liver Tumors (H. Remmer, H. M. Bolt, T. Bannash, and H. Popper, Eds.), University Park Press, Baltimore, 1978, pp. 261-283.
12. Jones, G., and Butler, W. H. Morphology of spontaneous and induced neoplasia. In: Mouse Hepatic Neoplasia (W. H. Butler, and P. M. Newberne, Eds.), Elsevier Publishing Co., New York, 1975, pp. 21-59.
13. Kyriazis, A. P., Koka, M., and Vesselinovitch, S. D. Metastatic rate of liver tumors induced by diethylnitrosamine in mice. Cancer Res. 34: 2881-2886 (1974).
14. Vesselinovitch, S. D., Mihailovich, N., and Rao, K. V., Morphology and metastatic nature of induced hepatic nodular lesions in C57BL × C3H F_1 mice. Cancer Res. 38: 2003-2010 (1978).
15. Vesselinovitch, S. D. Infant mouse as a sensitive bioassay system for carcinogenicity of *N*-nitroso compounds. In: *N*-Nitroso Compounds: Analysis, Formation, and Occurrence (E. A. Walker, L. Griciute, M. Castegnaro and M. Borzsony, Eds.), IARC Scientific Publ. 31, International Agency for Research on Cancer, Lyon, 1980, pp. 645-653.
16. Vesselinovitch, S D., Mihailovich, N., and Rao, K. V. N. Dose dependent rate of induction of hepatocellular carcinoma following single administration of diethylnitrosamine. Proc. Am. Assoc. Cancer Res. 21: 101 (1980).
17. Nomura, T. Timing of chemically induced neoplasia in mice revealed by the anti-neoplastic action of caffeine. Cancer Res. 40: 1332-1340 (1980).
18. Shimkin, M. B., and Polissar, M. J. Some quantitative observations on the induction and growth of primary pulmonary tumors in strain A mice receiving urethan. J. Natl. Cancer Inst. 16: 75-97 (1955).
19. Maskens, A. P. Confirmation of the two-step nature of chemical carcinogenesis in the rat colon adenocarcinoma model. Cancer Res. 41: 1240-1245 (1981).

20. Barka, T., and Anderson, P. J. Histochemistry—Theory, Practice and Bibliography. Harper and Row Publishers, New York, 1963.
21. Wachstein, M. and Meisel, E. On the histochemical demonstration of glucose-6-phosphatase. J. Histochem. Cytochem. 4: 592 (1956).
22. Chalkley, H. W. Method for quantitative morphologic analysis of tissues. J. Natl. Cancer Inst. 32: 1-17 (1964).
23. Goldfarb, S., and Pugh, T. D. The origin and significance of hyperplastic hepatocellular islands and nodules in hepatic carcinogenesis. J. Environ. Pathol. Toxicol. 1: 119-144 (1982).
24. Reuber, M. D. Transplantation studies. In: Mouse Hepatic Neoplasia (W. H. Butler and P. M. Newberne, Eds.), Elsevier Publishing Co., New York, 1975, pp. 141-153.
25. Koss, L. G. In: Diagnostic Cytology and Its Histopathologic Bases. Vol. 1, 3rd ed. Lipincott, Philadelphia, 1979, p. 76.
26. Nowell, P. C. The clonal evolution of tumor cell populations. Science 194: 23-28 (1976).
27. Farber, E., and Cameron, R. The sequential analysis of cancer development. Adv. Cancer Res. 31: 125-226 (1980).
28. Steel, G. G. Growth Kinetics of Tumors, Clarendon Press, Oxford, 1977, pp. 13-33.
29. Pitot, H. C., Goldsworthy, T., Campbell, H. A., and Poland, A. Quantitative evaluation of the promotion by 2,3,7,8-tetrachlorodibenzo-*p*-dioxin of hepatocarcinogenesis from diethylnitrosamine. Cancer Res. 40: 3616-3620 (1980).
30. Hennig, A., and Elias, H. A rapid method for the visual determination of size distribution of spheres from the size distributions of their sections. J. Microscopy 93: 101-107 (1970).
31. Elias, H., Hennig, A., and Schwartz, D. E. Stereology: application to biomedical research. Physiol. Rev. 51: 158-200 (1971).
32. Ogawa, K., Solt, D. B., and Farber, E. Phenotypic diversity as an early property of putative preneoplastic hepatocyte populations in liver carcinogenesis. Cancer Res. 40: 725-733 (1980).
33. Teebor, G. W., and Becker, F. F. Regression and persistence of hyperplastic hepatic nodules induced by *N*-2-fluorenylacetamide and their relationship to hepatocarcinogenesis. Cancer Res. 31: 1-3 (1971).
34. Hoover, K. L., Ward, J. M. and Stinson, S. F. Histopathologic differences between liver tumors in untreated (C57BL/5 × C3H) F_1 (B6C3 F_1) mice and nitrofen-fed mice. J. Natl. Cancer Inst. 65: 937-948 (1980).
35. Gellatly, J. B. The natural history of hepatic parenchymal nodule formation in a colony of C57BL mice with reference to the effect of diet. In: Mouse Hepatic Neoplasia (W. H. Butler and P. M. Newberne, Eds.) Elsevier Publishing Co., New York, 1975, pp. 77-108.
36. Goldfarb, S., Pugh, T. D., and Cripps, D J. Increased alkaline phosphatase activity—a positive histochemical marker for griseofulvin-induced mouse hepatocellular nodules. J. Natl. Cancer Inst. 64: 1427-1433 (1980).
37. Reuber, M. D. Histogenesis of hyperplasia and carcinomas of the liver arising around central veins in mice ingesting chlorinated hydrocarbons. Pathol. Microbiol. 43: 287-298 (1975).
38. Ward, J. M., Bernal, E., Buratto, B., Goodman, D. G., Standberg, J. D., and Schueler, R. Histopathology of neoplastic and non-neoplastic hepatic lesions in mice fed diets containing tetrachlorvinphos. J. Natl. Cancer Inst. 63: 111-117 (1979).
39. Shinozuka, H., Lombardi, B., Sell, S., and Iammarino, R. M. Early histological and functional alterations in rats fed a choline-deficient diet. Cancer Res. 38: 1092-1098 (1978).
40. Goldfarb, S., Vesselinovitch, S. D., Pugh, T. D., Mihailovich, N., Koen, H., and He, Y. Z. Remarkable uniformity of premalignant and malignant hepatocellular foci after single dose injection of diethylnitrosamine (DEN) in infant mice. Gastroenterology 79: 1021 (1980).
41. Goldfarb, S., Vesselinovitch, S. D., Pugh, T. D., Mihailovich, N., Koen, H., and He, Y. Z. Progression during early stages of mouse hepatocarcinogenesis in mice injected with diethylnitrosamine during infancy. Proc. Am. Assoc. Cancer Res. 22: 124 (1981).
42. Moore, M. P., Drinkwater, N. R., Miller, E. C., Miller, J. A., and Pitot, H. C. Quantitative analysis of the time-dependent development of glucose-6-phosphatase-deficient foci in the livers of mice treated neonatally with diethylnitrosamine. Cancer Res. 41: 1585-1593 (1981).